Applied Catalysis B: Environmental 182 (2016) 385–391

Contents lists available at ScienceDirect

Applied Catalysis B: Environmental

journal homepage: www.elsevier.com/locate/apcatb

Partial oxidation of methane over Ni^0/La_2O_3 bifunctional catalyst III. Steady state activity of methane total oxidation, dry reforming, steam reforming and partial oxidation. Sequences of elementary steps

Tri Huu Nguyen [a,b,c,*], Agata Łamacz [a,**], Andrzej Krztoń [a,1], Barbara Liszka [a], Gérald Djéga-Mariadassou [d,2]

[a] Centre of Polymer and Carbon Materials Polish Academy of Sciences, M. Curie-Skłodowskiej 34, 41-819 Zabrze, Poland
[b] Silesian University of Technology, Faculty of Chemistry, M. Strzody 9, 44-100 Gliwice, Poland
[c] Saigon University, Faculty of Pedagogy of Natural Sciences, 273 An Duong Vuong Dist.5, HCMC, Viet Nam
[d] University Pierre et Marie Curie, Paris, France

ARTICLE INFO

Article history:
Received 7 June 2015
Received in revised form 19 August 2015
Accepted 5 September 2015
Available online 11 September 2015

Keywords:
Bifunctional catalyst
Catalytic cycle
POM
Elementary steps

ABSTRACT

The bifunctional Ni^0/La_2O_3 catalyst was studied in the partial oxidation of methane (POM). The indirect model of POM was established based on catalytic runs of total oxidation of methane (TOM), dry reforming (DRM) and steam reforming (SRM). It was proved that TOM occurs over La_2O_3 (as well in flowing POM feed), whereas DRM and SRM take place over Ni^0. The sequences of elementary steps of each reaction are described based on previously published data from other authors. The reaction of total oxidation of methane supplies H_2O and CO_2 to SRM and DRM respectively. Therefore, SRM and DRM catalytic cycles are assisted by TOM whereas DRM and SRM are kinetically coupled on reduced metal active sites (Ni^0).

1. Introduction

This work is the third part of our study "Partial oxidation of methane (POM) on bifunctional Ni^0/La_2O_3 catalyst". In our first paper [1], the synthesis of Ni^0/La_2O_3 catalyst has been presented via the in situ transformation of $LaNiO_3$ under flowing POM mixture. An indirect model of POM reaction over the bifunctional Ni^0/La_2O_3 catalyst has been described (Fig. 1). In this model, total oxidation of methane (TOM) is kinetically assisting dry reforming (DRM) and steam reforming (SRM) cycles, which are kinetically coupled.

In this paper, elementary steps of methane total oxidation (TOM), dry reforming (DRM), steam reforming (SRM) and partial oxidation (POM) processes over Ni^0/La_2O_3 are described.

Total oxidation of methane. The mechanism of total oxidation of hydrocarbons on oxide catalysts is based on the theory of Haber and co-workers [2,3] and on the mechanism of Mars and van Krevelen [4]. Toops et al. [5] studied the kinetics of methane combustion over La_2O_3 and γ-Al_2O_3. To derive the rate equation on La_2O_3 they considered the mechanism of methane combustion with the formation of methyl radicals as a rate-determining step, the same model being also appropriate for Al_2O_3.

Surface reactions involving the formation of methyl radicals and their subsequent reaction with oxygen are far equilibrium and considered as a "one-way" step, according to Boudart and Djéga-Mariadassou [6-p.90]. Dissociative O_2 adsorption on La_2O_3 has been previously verified [7].

Haber and Witko [2] have shown that the activation of methane on V_2O_5 occurs owing to a C—H bond cleavage leading to surface OCH_3 and OH groups as presented Fig. 2. This figure shows the surface first layer of the periodic boundary model of V_2O_5 (010) [8] and the interaction of V_2O_5 with isolated CH_3 and H adsorbed species obtained after CH_4 activation by homolytic cleavage of the C—H bond [2]. They bond to oxygen being in the nearest neighborhood.

According to Haber and Turek [3], it is also very important to emphasize that for the total oxidation of methane to CO_2/H_2O occurring on a metal oxide "MO", CO is not an intermediate of reaction.

* Corresponding author at: Centre of Polymer and Carbon Materials Polish Academy of Sciences, M. Curie-Skłodowskiej 34, 41-819 Zabrze, Poland .
** Corresponding author.
E-mail addresses: huutri_sgu@yahoo.com (T.H. Nguyen), agata.lamacz@cmpw-pan.edu.pl (A. Łamacz).
[1] Died on August 13th 2015.
[2] On leave from UPMC.

http://dx.doi.org/10.1016/j.apcatb.2015.09.016
0926-3373/

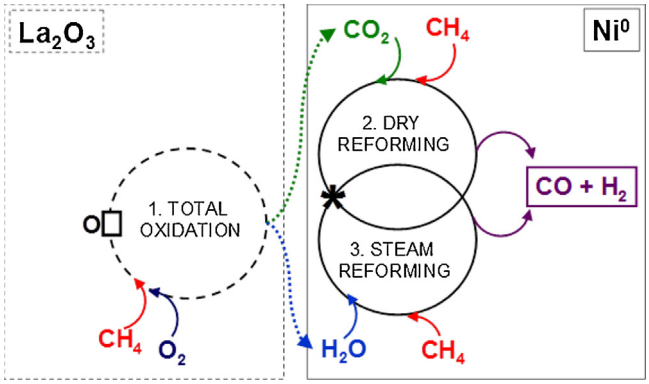

Fig. 1. Model of POM reaction according to [1], where "O□" is the active site of La_2O_3; "*" is the surface Ni^0 atom.

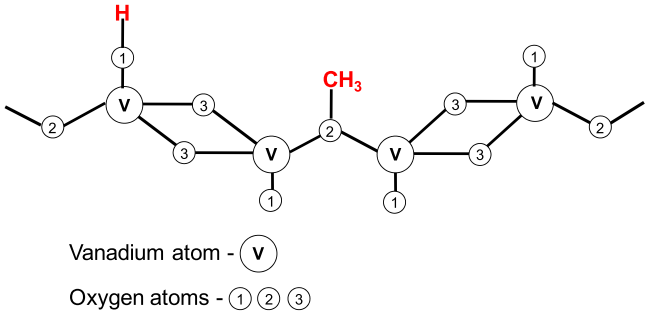

Fig. 2. Scheme of OCH_3 and OH species on the surface of V_2O_5 resulting from the dissociative adsorption of methane on the oxide surface according to [8].

Dry and steam reforming of methane. Several publications have been published on this topics [9–27]. Two general models, direct and indirect ones, have been considered. Let's note that reforming reactions are occurring over the reduced metallic sites "M^0".

The indirect pathway can be first considered. Rostrup-Nielsen and Bak Hansen [9] had performed the reforming of methane with CO_2 and H_2O over transition metals catalyst, i.e. on Ni, Ru, Rh, Pd and Ir supported on magnesia. They suggested that the mechanism of CO_2 reforming over metal-based catalysts does not differ significantly from that of steam reforming. The authors proposed that in both processes total dehydrogenation of CH_4 is occurring over M^0, which leads to [M-CH_{4-x} + xM-H] where x equals from 0 to 4, and is followed by reaction with surface O species, originating either from CO_2 or H_2O. Qin et al. [10,11] qualitatively confirmed the work of Rostrup Nielsen and Bak-Hansen. Similarly, Wei and Iglesia studied the mechanism and kinetics of dry and steam reforming of methane over (Pt, Ru, Ni)/MgO [12–14] and Rh/Al_2O_3 or Rh/ZrO_2 [15]. These authors suggested the same elementary steps for dry reforming and steam reforming over selected supported metals. Furthermore Wei and Iglesia [14,15], Bradford and Vannice [16] always noted the occurrence of water gas shift reaction. According to Zhang and Verykios [17], La_2O_3 itself exhibits negligible reactivity towards DRM.

Maestri et al. [18] have established a hierarchy between the different kinetic models of methane conversions (steam and dry reforming) by a microkinetic approach including water-gas shift and reverse water gas shift reactions. The authors have included all the adsorption/desorption steps of the molecular species. Likewise, Maier et al. [19] have detailed a multi-step reaction mechanism for modelling the steam reforming of methane over nickel-based catalysts.

In the direct model of DRM, the metal-oxide interface has been considered for defining active sites at the Ni–La_2O_3 interface [20], or at the Pt–ZrO_2 perimeter [21]. Bradford and Vannice [22] also concluded that active sites are created in the Pt–TiO_x interfacial region. The dual site mechanism proposed by Schmal and co-authors [23,24] over supported Rh on lanthanum-based solid is including the dehydrogenation of CH_4 on metal particles and CO_2 activation on the support. Also in the direct model of DRM involving the metal–support interface, Tsipouriari and Verykios [25] concluded that formation of oxycarbonate species during reaction plays a central role in dry reforming of methane over Ni/La_2O_3. CH_4 decomposes on nickel crystallites to yield H_2, whereas adsorbed carbon reacts with oxycarbonate at the interface to release CO.

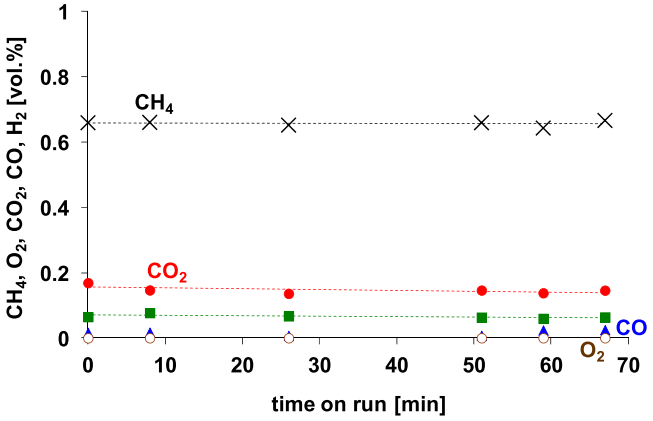

Fig. 3. TOM over La_2O_3 at 1073 K ($CH_4/O_2/Ar$ = 0.9/ 0.5/98.6 vol.%). CH_4 (×), O_2 (o), CO_2 (●), CO (▲), H_2 (■).

Concerning the extrapolation of laboratory-scale experiments, Resasco and co-authors [26] have concluded that studies conducted at lower temperatures can be invalid for the dry reforming reaction at high temperature. Concerning hydroxyl groups formation it has been shown [27] that these species may not play a significant role under industrial conditions.

Reliable global kinetic values (power rate law equations) of methane total oxidation and dry reforming have been calculated in our previous paper [28]. Experimental rate constants, partial orders to reactants, activated energies of TOM over La_2O_3, DRM and POM over Ni^0/La_2O_3 have been determined. Furthermore the rate determining cycle (rdc) of POM, that is the slower cycle turning over in the frame of our model (Fig. 1) has been shown to be the TOM cycle. The goal of this paper is to describe the detailed sequences of elementary steps of the three reactions occurring in the indirect model of POM (Fig. 1) based on the mechanisms suggested above in this section by several authors [3–5,10–15]. In order to further justify the model, we have separately studied the total oxidation of methane (TOM) over La_2O_3 alone (1st function) under flowing POM mixture. Then DRM, SRM (2nd function) and POM reactions were separately studied over Ni^0/La_2O_3 catalyst. The sequence of elementary steps of catalytic TOM will be described via the model proposed by Haber et al. [2,3]. The sequence of elementary steps of catalytic DRM and SRM reactions will be also described based on elementary steps already described by several authors [9–19].

2. Experimental

2.1. Synthesis of Ni^0/La_2O_3 catalyst

The lanthanum oxide supported nickel catalyst (Ni^0/La_2O_3) was synthesized from $LaNiO_3$ perovskite precursor. The procedure of $LaNiO_3$ synthesis and its in situ transformation by the POM reaction mixture (CH_4/O_2 = 2) to Ni^0/La_2O_3, have been described in details in our previous paper [1].

2.2. Catalytic tests

The catalytic runs of TOM, DRM, SRM and POM reactions were carried out in stationary conditions (isotherms). The reaction of TOM was conducted over La_2O_3 in the POM mixture, i.e. 1 vol.% CH_4 + 0.5 vol.% O_2 (POM stoichiometric gas mixture) and Ar as balance. The catalytic runs of DRM, SRM and POM reactions were carried out over Ni^0/La_2O_3 catalyst in the mixtures containing (i) 0.7 vol.% CH_4 + 0.7 vol.% CO_2 in Ar, (ii) 1 vol.% CH_4 + 1 vol.% H_2O in Ar and (iii) 1 vol.% CH_4 + 0.5 vol.% O_2 in Ar, respectively.

All experiments were performed at atmospheric pressure, in a continuous flow of reaction mixtures, in a fixed bed U-shape quartz reactor of 18 mm inner diameter. The reaction was carried out at 1073 K. The catalyst weight was 0.2 g for the TOM tests and 0.3 g for DRM, SRM and POM. The total flow rate was 100 ml/min. The substrates and products were analyzed using a gas chromatograph (GC) equipped with a thermal conductivity detector (TCD).

3. Results and discussion

3.1. Function 1 of the bifunctional catalyst: methane total oxidation under flowing POM mixture over La_2O_3, in steady state conditions at 1073 K

The aim of this study was to demonstrate that in the presence of POM mixture, the only reaction occurring over La_2O_3 is the total oxidation of methane (TOM):

$$CH_4 + 2O_2 = CO_2 + 2H_2O \quad (1)$$

The composition of the gas mixture after TOM reaction over La_2O_3 is reported in Fig. 3. On this basis, the following observations have been made:

(i) In this experiment, about 28% conversion of methane is observed, whereas oxygen is completely consumed. The real - composition of the initial reaction mixture (CH_4:O_2 = 0.9:0.5; in practice, the methane concentration was only 0.9 vol.% instead of 1 vol.% in this experiment) and the composition of reagents/products, at the steady state, are expected to be as follows: CH_4: O_2:CO_2 = 0.65:0: 0.25 (water was not measured).

(ii) The amount of CH_4 is consistent with the above-expected result, but the amount of CO_2 is only 0.17 vol.%. According to literature, adsorbed carbonates species [29,30], subsequently leading to the formation of bulk $La_2O_2CO_3$, can occur at 1073 K.

(iii) The presence of about 0.08 vol% of H_2 can be due to H_2O dissociation over oxygen vacancies (□) on the surface of La_2O_3 according to (Eq. (2)), as it has been observed to occur over CeO_2 or $CeZrO_2$ [31,32]:

$$H_2O + \square => \square O + H_2 \quad (2)$$

(iv) The very small formation of CO can be due to the reverse water gas shift reaction (RWGS). Furthermore, from the 22nd to 51st minute of test run, the amount of CO is practically near 0. Therefore, it can be concluded that if there is no H_2–CO mixture, which are the molecular proof for reforming of methane, La_2O_3 is inactive in DRM and SRM reactions [1]. Zhang and Verykios [17] have also found that La_2O_3 exhibits negligible reactivity towards DRM.

Therefore, it is proven that La_2O_3 fulfills the first function of Ni^0/La_2O_3 in the overall POM process, catalyzing TOM reaction Eq. (1).

3.1.1. Sequence of elementary steps defining the catalytic cycle of the total oxidation of CH_4

On the basis of the above results and already published papers [2,3,33], the following sequence of elementary steps of TOM can be considered:

"La - □" stands for the active site at the surface of La_2O_3 with O vacancy (□), and

"La – O" is the site with surface oxygen = O^- (electrophilic species according to Haber and Turek [3])

				σ	
[1]	CH_4 + La-O	→ {CH_4}····O-La	k_1	1	(3)
[2]	{CH_4}····O-La + La-O	→ CH_3O-La + La-OH	k_2	1	(4)
[3]	CH_3O-La	→ ….	k_3	1	(5)
	(other unspecified, kinetically no significant steps leading to the reaction products CO_2 and H_2O) [34-p. 98]				
[4]	2 La-□ + O_2	→ 2 La-O	k_4	2	(6)
	Overall equation: $CH_4 + 2O_2 = CO_2 + 2H_2O$				(1)

Step 1 corresponds to the first activation of methane with the formation of a surface complex between one surface oxygen and CH_4.This step is justified by the order observed to methane in the global kinetic approach [28], showing that there is no direct dissociative adsorption of methane over two La-O active sites.

Step 2 corresponds to the 2nd step of dissociative adsorption of methane owing to the proximity of an adjacent "La-O" surface active site. Step 1 and step 2 are consistent with Haber et al. model pathway of methane activation [2].

Step 3 is the beginning of the oxidation of adsorbed methoxy groups; being reactive and consequently at low concentration, they are not the "most abundant reactive intermediate" (mari) [6,34].

Step 4 is the end of the oxidation process and leads to O_2 dissociative adsorption over two adjacent surface oxygen vacancies "La-□". This step is required, according to Mars and Van Krevelen's mechanism [4], to the recovering of the active site [La-O] necessary for the catalytic cycle to turnover.

The catalytic cycle of TOM over La_2O_3 is therefore defined by Fig. 4.

3.2. Function 2 of the bifunctional catalyst: methane reforming reaction at 1073 K over Ni^0/La_2O_3

3.2.1. Dry reforming of methane on Ni^0/La_2O_3 in steady state at 100% conversion of reactants conditions

The catalytic run of DRM reaction over Ni^0/La_2O_3 is reported in Fig. 5. Methane and carbon dioxide were almost completely consumed. Considering the experimental ratio H_2/CO near 1 and the absence of CO_2, it can be considered that WGS reaction is not occurring. Methane conversion and formation of CO and H_2 were stable up to 4 h of test run. The H_2/CO ratio is 1.05 which corresponds to the theoretical H_2/CO ratio Eq. (7).

$$CH_4 + CO_2 = 2CO + 2H_2 (H_2/CO = 1) \quad (7)$$

The amount of CO is smaller (by 3%) than the amount of introduced carbon (CH_4 + CO_2), this can be due to small deposition of some carbon species on the catalyst surface. It will be discussed later, in the sequence of elementary steps of DRM, by the total dehydrogenation of methane to adsorbed active carbon over Ni^0. The above results prove that Ni^0/La_2O_3 is active in DRM. This is in agreement with the results obtained for this catalyst by Gallego et al. [35]. Tsipouriari et al. [25] and Zhang et al. [20] had stud-

ied the DRM reaction over Ni^0/La_2O_3 at 973 K. They observed 90% conversion of hydrocarbon and H_2/CO ratio close to 1 during 100 h catalytic run. Neither RWGS nor carbon deposition were occurring.

3.2.2. Sequence of elementary steps of methane dry reforming reaction.

How is the DRM reaction occurring at the molecular level? It can be described according to the sequence of elementary steps [9–15,18,19], with their stoichiometric number "σ" [6].

Methane activation ("dehydrogenation"): σ

$CH_{4(gas)} + 2* \rightarrow CH_3* + H*$ 1 (8)

$CH_3* + * \rightarrow CH_2* + H*$ 1 (9)

$CH_2* + * \rightarrow CH* + H*$ 1 (10)

$CH* + * \rightarrow C* + H*$ 1 (11)

CO_2 activation:

$CO_2 + * \rightarrow CO_2*$ 1 (12)

$CO_2* + * \rightarrow CO* + O*$ 1 (13)

$CO* \rightarrow CO + *$ 1 (14)

Surface reactions:

$C* + O* \rightarrow CO* + *$ 1 (15)

$CO* \rightarrow CO + *$ 1 (14)

$H* + H* \rightarrow H_2 + 2*$ 2 (16)

$CH_4 + CO_2 = 2CO + 2H_2$ *(overall reaction)* **$H_2/CO = 1$** (7)

Methane dehydrogenates step by step Eqs. (8)–(11) [13,14] what, at the end, leads to active carbon (*C) and hydrogen species (*H) adsorbed on metallic active site "*", i.e. Ni^0. CO_2 decomposes to CO and adsorbed oxygen (O*) Eqs. (12)–(14). Subsequently, C* is oxidized to CO* with adsorbed *O, Eq. (15). In the next step CO* desorbs as $CO_{(g)}$ Eq. (14), and two H* species react to form H_2 Eq. (16). Hence, the active sites (*) are recovered, and this is a fundamental role of catalysis [34].

Let's note that a deposition of carbon from DRM (or SRM) mechanism can occur when the oxidation of this active carbon adsorbed on Ni^0 Eq. (12) is not subsequently and rapidly oxidized by an adjacent *O coming from CO_2 (or H_2O for SRM) Eqs. (13–15).

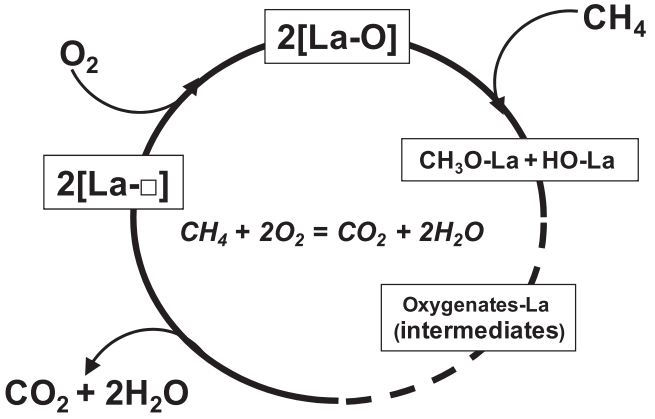

Fig. 4. Catalytic cycle with elementary steps of methane total oxidation.

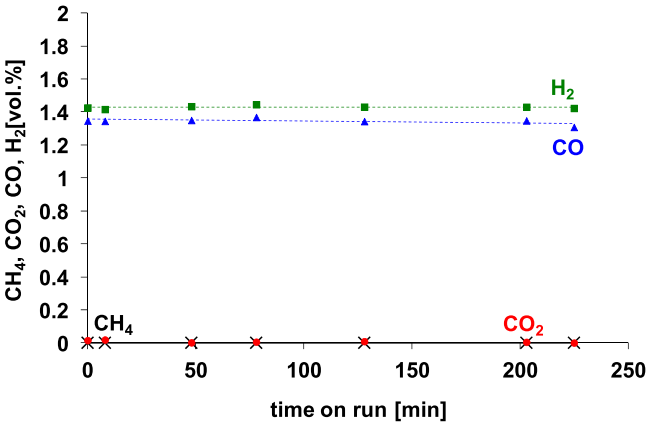

Fig. 5. DRM on Ni^0/La_2O_3 at 1073 K ($CH_4/CO_2/Ar = 0.7/0.7/98.6$ vol.%). CH_4 (×), CO_2 (●), CO (▲), H_2 (■).

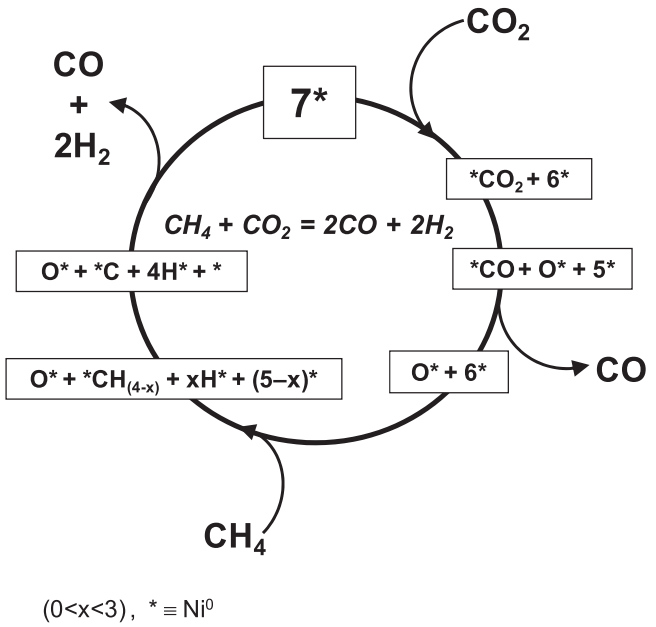

Fig. 6. Catalytic cycle with the elementary steps of methane dry reforming.

The catalytic cycle of DRM (based on classical kinetics) is presented Fig. 6. It takes into account the stoichiometric number of each elementary step. According to the assumptions of catalysis, the active sites are recovered within the catalytic cycle.

Let's note that the numbers 7* (Fig. 6) or 6* (Fig. 8) of the catalytic cycles are not the number of Ni^0 atoms defining the active sites but, according to Boudart's school, the total number of surface unique atoms of Ni^0 working in the whole sequence of elementary steps. It can be seen that only 1* or 2* are used in a given elementary step.

3.2.3. Steam reforming of methane on Ni^0/La_2O_3 in steady state at 100% conversion of reactants conditions

The overall reaction of SRM is described by Eq. (17).

$$CH_4 + H_2O = CO + 3H_2 (H_2/CO = 3) \quad (17)$$

The result of SRM run, carried out at 1073 K over Ni^0/La_2O_3 catalyst is presented in Fig. 7.

It can be observed that methane conversion was close to 100% and formations of CO and H_2 were stable up to 4 h of test run.

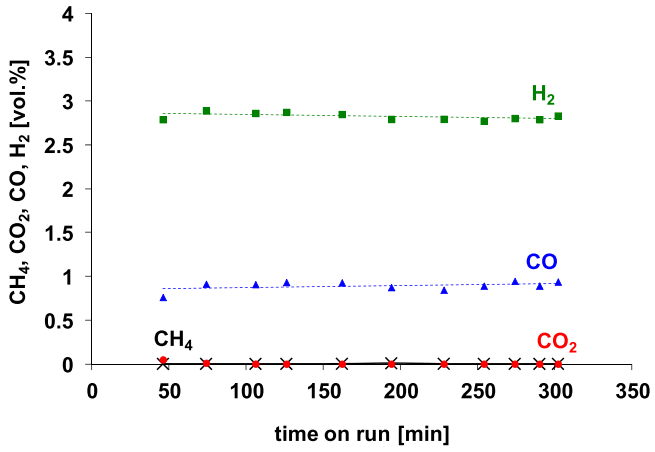

Fig. 7. SRM on Ni^0/La_2O_3 at 1073 K ($CH_4/H_2O/Ar = 0.9/1/98.1$ vol.%). CH_4 (×), CO_2 (●), CO (▲), H_2 (■).

The H_2/CO ratio was 3.2, therefore close to the theoretical ratio of 3 according to Eq. (17). No CO_2 was detected in the reactor outlet thus proving that the WGS reaction was not occurring in the experimental conditions of SRM. The obtained results are in agreement with those presented by other authors [36,37]. The absence of WGS probably arises from low steam to carbon ratio (S/C = 1) and high temperature of experiment (thermodynamic limitation of this reaction) [37]. Provendier et al. [38] performed the catalytic run of SRM over the pre-reduced $LaNiO_3$, producing Ni^0/La_2O_3. The SRM was carried out at 1073 K with S/C = 1. The authors observed that Ni^0/La_2O_3 deactivated rapidly due to a significant carbon deposition. Pereniguez et al. [39] studied both DRM and SRM at 1073 K over $LaNiO_3$ perovskite precursor. In their studies, the catalyst was pre-reduced in situ by reaction mixtures. The authors have observed methane conversion of 75% during SRM and high deactivation of the catalyst. In contrary, the performance of this catalyst in DRM was much better (90% of methane conversion) and remained unchanged even after 12 h of the test run. It means that the catalyst is more stable under DRM than SRM conditions. The authors' SEM observations of the catalyst after DRM and SRM did not show the presence of significant amounts of carbon deposits. Therefore, the authors suggested that different deactivation behavior of the catalyst in DRM and SRM could be related to some changes in the metallic phase, which were induced by reaction conditions. Urasaki et al. [40] studied methane SRM over 10% Ni supported on various perovskites ($LaFeO_3$, $BaTiO_3$, $SrTiO_3$, $LaAlO_3$). The catalytic runs were carried out at 1073 K, under atmospheric pressure and at S/C = 2. They observed a correlation between CH_4 conversion and activity of the catalysts. This was attributed to the size of nickel particles, and the type of support. It has been found out that H_2O excess provided the regeneration of the initial structure of perovskite but nickel has not been oxidized.

According to the above cited literature data and results presented in this paper, we can conclude that the in situ transformation of $LaNiO_3$ (in our case by POM reaction mixture [1]) to Ni^0/La_2O_3 provides high activity in SRM. The obtained results proved that zero valent nickel atom is the active site for SRM reaction, and as was mentioned in Section 3.1, La_2O_3 was not able to catalyze reforming reactions.

3.2.4. Sequence of elementary steps and catalytic cycle of methane steam reforming reaction

The SRM over Ni^0/La_2O_3 occurs in a similar way than that of DRM (presented in Section 3.2.2).

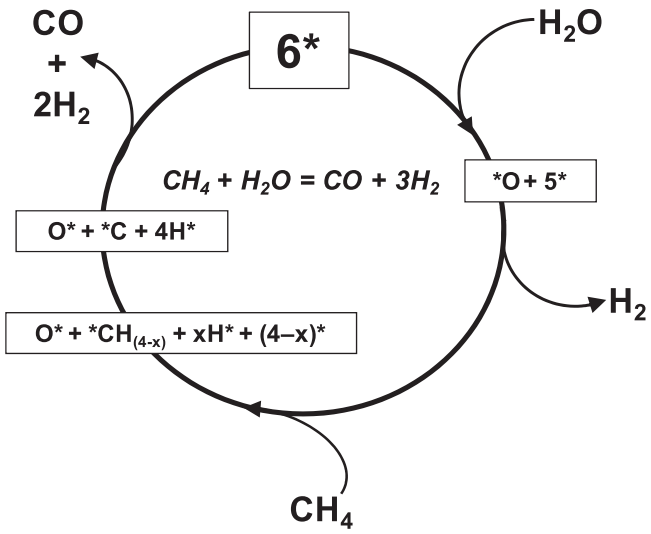

Fig. 8. Catalytic cycle and elementary steps of methane steam reforming.

Methane activation (said "dehydrogenation"):		σ	
$CH_{4(gas)} + 2^* \rightarrow CH_3^* + H^*$		1	(8)
$CH_3^* + ^* \rightarrow CH_2^* + H^*$		1	(9)
$CH_2^* + ^* \rightarrow CH^* + H^*$		1	(10)
$CH^* + ^* \rightarrow C^* + H^*$		1	(11)
H_2O activation:			
$H_2O + ^* \Rightarrow H_2 + O^*$		1	(18)
Surface reactions:			
$C^* + O^* \rightarrow CO^* + ^*$		1	(15)
$CO^* \rightarrow CO + ^*$		1	(14)
$H^* + H^* \rightarrow H_2 + 2^*$		2	(16)
$CH_4 + H_2O = CO + 3H_2$	*(overall reaction)*	**$H_2/CO = 3$**	(17)

Let's note that H_2O dissociative adsorption can occur according to the following 3 elementary steps, similarly to precious metals:

$H_2O + 2^* \rightarrow HO^* + H^*$	σ=1	(19)
$HO^* + ^* \rightarrow O^* + H^*$	σ =1	(20)
$2H^* \rightarrow H_2 + 2^*$	σ =1	(16)
Overall equation: $H_2O + ^* \Rightarrow O^* + H_2$		(18)

In this case the water dissociation is no more an elementary step.

Likewise in the case of DRM, during SRM, methane dehydrogenates on Ni^0 ("*") to C^* and H^* Eqs. (8)–(11). The H_2O adsorbs and dissociates on the metal "*" active sites, yielding H_2 and O^* Eq. (18), which subsequently oxidizes C^* to CO^* Eq. (15). Desorption of CO Eq. (14) and H_2 Eq. (16) leads to the recovery of active sites.

The sequence of elementary steps and the corresponding catalytic cycle of SRM is shown in Fig. 8.

These sequence of elementary steps clearly evidences that the process of methane activation is the same as for DRM. This important feature will lead to the conclusion that the rates of DRM and SRM are the same, which is also generally accepted in literature [12–14,41].

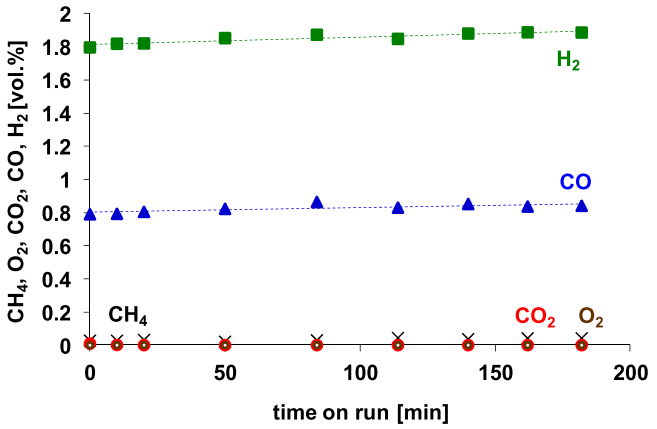

Fig. 9. POM reaction on Ni^0/La_2O_3 at 1073 K ($CH_4/O_2/Ar = 0.9/0.5/98.5$ vol.%). CH_4 (×), O_2 (○), CO_2 (●), CO (▲), H_2 (■).

3.3. Partial oxidation of methane on Ni^0/La_2O_3 in steady state

The reaction is described by Eq. (21) and results of catalytic run are presented in Fig. 9.

$$CH_4 + ½O_2 = CO + 2H_2 \quad (21)$$

It can be observed that CH_4 and O_2 were almost completely consumed. The methane conversion was stable during the experiment and the H_2/CO ratio was 2.2, which was higher than that arising from stoichiometry of POM Eq. (21). It can be due to (i) the lack of carbon for CO formation, mainly caused by formation of carbonates over La_2O_3 [29,30] (as explained in Section 3.1), or (ii) carbon deposit in reaction of methane dehydrogenation Eqs. (8)–(11) and subsequent migration of *C on the support.

According to Fig. 1, which presents how is POM reaction occurring, three reactions (TOM + DRM + SRM) have to turn over simultaneously. The TOM reaction leads to CO_2/H_2O and occurs on La_2O_3. We have reported [1] that oxygen from the gas phase is completely consumed in TOM catalytic cycle of POM process. Methane not consumed in TOM, is converted to CO and H_2 in DRM and SRM, both occurring on Ni^0 active sites. The TOM cycle has no common intermediate species with DRM and SRM, but it provides oxidizing agents, i.e. CO_2 and H_2O to DRM and SRM, respectively. Hence, the catalytic cycles of DRM and SRM are assisted by TOM catalytic cycle. However, DRM and SRM catalytic cycles have common intermediate species, i.e. O*, which is coming from CO_2 or H_2O. In classical kinetics, it is called a kinetic coupling [6].

4. Conclusion

The Ni^0/La_2O_3 catalyst used in this work is a bifunctional catalyst. Its two functions are:

1) Methane total oxidation to carbon dioxide and water occurring over La_2O_3,
2) Reforming reactions (DRM/SRM) occurring over Ni^0.

The pathway of each reaction at the molecular level is described. The sequences of elementary steps at the molecular level for each catalytic cycle are presented. The present work shows in details catalytic cycles of POM process. The kinetic coupling of DRM and SRM over Ni^0 (*) active site is proved by the catalytic runs of each reaction alone. These reactions are kinetically coupled through the zero valent metal active site (Ni^0). Products of POM reaction, i.e. H_2 and CO, originate from:

1) Methane dehydrogenation producing active carbon *C and H_2,
2) Dissociation of H_2O and CO_2 (products of TOM reaction) producing *O, H_2, and CO,
3) Subsequent oxidation of *C by *O, leading to CO.

Since the reaction of methane total oxidation supplies H_2O and CO_2 to SRM and DRM respectively, SRM and DRM catalytic cycles are assisted by TOM.

The Ni^0/La_2O_3 catalyst has shown a good activity in DRM, SRM and POM reactions. The secondary reactions, such as WGS or RWGS, did not occur during DRM, SRM and POM at 1073 K in our experimental conditions.

Acknowledgements

Dr. M. Lewandowski is greatly acknowledged for providing lanthanum oxide material.

The Institute of General and Ecological Chemistry of Lodz University of Technology is gratefully acknowledged for support to Tri Huu Nguyen to do global kinetics (power rate laws) of TOM and DRM.

The government of Vietnam is gratefully acknowledged for the grant (4915/QD-BGDDT) given to Tri Huu Nguyen to realize this work in Poland.

References

[1] T.H. Nguyen, A. Łamacz, P. Beaunier, S. Czajkowska, M. Domański, A. Krztoń, T.V. Le, G. Djéga-Mariadassou, Appl. Catal. B 152–152 (2014) 360.
[2] J. Haber, M. Witko, J. Catal. 216 (2003) 416.
[3] J. Haber, W. Turek, J. Catal. 190 (2000) 320.
[4] P. Mars, D.W. van Krevelen, Chem. Eng. Sci. 3 (1954) 41.
[5] T.J. Toops, A.B. Walters, M.A. Vannice, Appl. Catal. A 233 (2002) 125.
[6] G. Djéga-Mariadassou, M. Boudart, J. Catal. 216 (2003) 89.
[7] S.-J. Huang, A.B. Walters, M.A. Vannice, Appl. Catal. B. 26 (2000) 101.
[8] X. Yin, H. Han, A. Miyamoto Phys, Chem. Chem. Phys. 2 (2000) 4243.
[9] J.R. Rostrup-Nielsen, J.-H. Bak Hansen, J. Catal. 144 (1993) 38.
[10] D. Qin, J. Lapszewicz, Catal. Today 21 (1994) 551.
[11] D. Qin, J. Lapszewicz, X. Jiang, J. Catal. 159 (1996) 140.
[12] J. Wei, E. Iglesia, J. Phys. Chem. B 108 (2004) 4094.
[13] J. Wei, E. Iglesia, J. Phys. Chem. B 108 (2004) 7253.
[14] J. Wei, E. Iglesia, J. Catal. 224 (2004) 370.
[15] J. Wei, E. Iglesia, J. Catal. 225 (2004) 116.
[16] M.C.J. Bradford, M.A. Vannice, Appl. Catal. A 142 (1996) 97.
[17] Z. Zhang, X.E. Verykios, Appl. Catal. A 138 (1996) 109.
[18] M. Maestri, D.G. Vlachos, A. Beretta, G. Groppi, E. Tronconi, J. Catal. 259 (2008) 211.
[19] L. Maier, B. Schädel, K.H. Delgado, S. Tischer, O. Deutschmann, Top. Catal. 54 (2011) 845.
[20] Z. Zhang, X.E. Verykios, S.M. MacDonald, S. Affrossman, J. Phys. Chem. 100 (1996) 744.
[21] J.H. Bitter, K. Seshan, J.A. Lercher, J. Catal. 171 (1997) 279.
[22] M.C.J. Bradford, M.A. Vannice, J. Catal. 173 (1998) 157.
[23] M.M.V.M. Souza, D.A.G. Aranda, M. Schmal, J. Catal. 204 (2001) 498.
[24] J.F. Múnera, S. Irusta, L.M. Cornaglia, E.A. Lombardo, D.V. Cesar, M. Schmal, J. Catal. 245 (2007) 25.
[25] V. Tsipouriari, X.E. Verykios, Catal. Today 64 (2001) 83.
[26] S.M. Stagg, E. Romeo, C. Padro, D.E. Resasco, J. Catal. 178 (1998) 137.
[27] K.S. Langner, K.J. Goldwasser, M. Houalla, D.M. Hercules, Catal. Lett. 32 (1995) 263.
[28] T.H. Nguyen, A. Łamacz, A. Krztoń, A. Ura, K. Chałupka, M. Nowosielska, J. Rynkowski, G. Djéga-Mariadassou, Appl. Catal. B 165 (2015) 389.
[29] G. Valderrama, A. Kiennemann, M.R. Goldwasser, Catal. Today 133–135 (2008) 142.
[30] G. Valderrama, M.R. Goldwasser, C. Urbina de Navarro, J. Barrault, J.M. Tatibouët, C. Batiot-Dupeyrt, F. Martinez, Catal. Today 107–108 (2005) 785.
[31] N. Laosiripojana, S. Assabumrungrat, Appl. Catal. B 60 (2005) 107.
[32] A. Lamacz, A. Krzton, Inter. J. Hydrogen Energy 38 (2013) 8772.
[33] S. Chempath, A.T. Bell, J. Catal 247 (2007) 119.
[34] (a) M. Boudart, G. Djéga-Mariadassou, Cinétique des Réactions en Catalyse Hétérogène, Masson et Cie, Paris, 1982;
(b) M. Boudart, G. Djéga-Mariadassou, Kinetics of Heterogeneous Catalytic Reactions, Princeton University Press, Princeton, NJ, 1984.

[35] G.S. Gallego, C.B. Dupeyrat, J. Barrault, F. Mondragon, Ind. Eng. Chem. Res. 47 (2008) 9272.
[36] H.S. Roh, K.W. Jun, W.S. Dong, S.E. Park, Y.S. Baek, Catal. Lett. 74 (2001) 1–2.
[37] D. Hufschmidt, L.F. Bobadilla, F.R. Sarria, M.A. Centeno, J.A. Odriozola, M. Montes, E. Falabella, Catal. Today 149 (2010) 394.
[38] H. Provendier, C. Petit, A. Kiennemann, C.R. Acad, Sci. Paris Serie IIc, Chimie/Chem. 4 (2001) 57.
[39] R. Pereniguez, V.M.G. DelaCruz, J.P. Holgado, A. Caballero, Appl. Catal. B 93 (2010) 346.
[40] K. Urasaki, Y. Sekine, S. Kawabe, E. Kikuchi, M. Matsukata, Appl. Catal. A 286 (2005) 23.
[41] A. Donazzi, A. Beretta, G. Groppi, P. Forzatti, J. Catal. 255 (2008) 259.